STRUCTURE AND PROPERTIES OF NANOSIZE NiFe$_2$O$_4$ PREPARED BY TEMPLATE AND PRECIPITATION METHODS

A. Ćosović [a], V. Ćosović [b,*], T. Žák [c], B. David [c], N. Talijan [b]

[a] Institute for Technology of Nuclear and Other Mineral Raw Materials, Belgrade, Serbia
[b] University of Belgrade, Institute of Chemistry, Technology and Metallurgy, Belgrade, Serbia
[c] CEITEC IPM, Institute of Physics of Materials AS CR, Brno, Czech Republic

Abstract

Nanosize NiFe$_2$O$_4$ was prepared by template method and precipitation process using same starting materials. The use of soluble starch in both synthesis routes was investigated. The amount of the used precipitating agent (Na$_2$CO$_3$) for the precipitation approach was selected according to two adopted scenarios based on theoretical and average yield of possible side reaction expressed by the degree of substitution (DS). The results of SEM microstructural analysis of the prepared Ni-ferrite powders demonstrate evident influence of the applied preparation method whereas high-magnification FE-SEM images show very similar fine-grained structures characterized by different size of particles. According to the results of XRD analysis, the obtained ferrite powders exhibit only slight differences in phase composition with calculated crystallite size for template sample d$_{XRD}$ = 36 nm and for the both precipitation route samples d$_{XRD}$ = 21 nm. Additional sample characterization using ^{57}Fe Mössbauer spectroscopy supports the findings of the microstructural and XRD analysis. The "clearest" spectrum was obtained for the template sample while the strongest influence of nanocrystalline component was observed for the sample prepared with maximal amount of precipitation agent (DS=3). The room temperature magnetic hysteresis loops, recorded using vibrating sample magnetometer (VSM), are very similar and exhibit characteristic shape with values of magnetic properties within expected range for this type of material.

Keywords: Nanosized NiFe$_2$O$_4$; Template method; Precipitation route; Microstructure; Phase composition; Magnetic properties.

1. Introduction

Nickel ferrite is rather important functional material, with wide field of application. Traditionally it has been extensively studied for application as a soft magnetic material. However, development of nanotechnology prompted new applications and opened new research areas. Among other uses, this material has been recently investigated for use in hydrogen production [1], as catalyst for CO$_2$ catalytic decomposition [2], as photo reactive material, and for gas sensing [3]. Studies suggest that morphology, crystal and particle sizes have significant influence on material's properties such as reactivity or affinity towards certain types of ions [3]. Therefore any practical application of the material based on these properties heavily depends on method of synthesis, since it has dominant influence on morphology. Over the years many innovative methods have been developed and employed to synthesize nickel ferrite nanoparticles. Methods like citrate precursor method [4], reactive milling [5], and several variations of hydrothermal method.

In this study, the use of soluble starch in synthesis of nanosized NiFe$_2$O$_4$ was investigated. Two different approaches were explored, but in both same starting materials were used. Nickel sulfate was used as precursor for nickel oxide, and ferric nitrate as precursor for ferric oxide. The first approach is a template method in which soluble starch is used as soft template and it is based on the properties of nickel sulfate and ferric nitrate to thermally decompose into corresponding oxides. The second approach is a precipitation process in which soluble starch is used as dispersing agent and sodium carbonate as a precipitating agent. Usually, sodium hydroxide is used for precipitation, however in this experiment sodium carbonate was chosen since it is often used for nickel removal process for environmental purposes as well in metal recovery processes, and since it is less aggressive than hydroxide. Generally, all reactants and template material were chosen to be cheap, easily accessible, and reasonably safe to work with.

2. Materials and methods

Analytical grade inorganic salts $NiSO_4 \cdot 6H_2O$ and $Fe(NO_3)_3 \cdot 9H_2O$ were used as precursors of nickel and ferric oxides. All chemical reagents used for the synthesis process, including soluble starch $(C_6H_{10}O_5)_n$ and anhydrous sodium carbonate (Na_2CO_3) were supplied by Merck. All chemicals were used directly without further purification.

2.1 Template method

Generally, template method includes three steps: template preparation, insertion of the precursors into the template (impregnation) and template removal. In this approach water solution of soluble starch was used as a soft template. When mixed with water solutions of inorganic salts, starch breaks up solution of inorganic salts into fine droplets confined within polymer chains. During the drying process it solidifies, entrapping the mixed salts crystals that form in droplets as water is being removed in a solid organic matrix. Size of the formed crystals is determined by the volume of droplets and concentration of inorganic salts in water solution. Combustion and latter calcination remove the organic matrix and transform salts crystals to oxides that will produce mixed oxide particles. The $NiFe_2O_4$ powder sample prepared by template route was labeled NF1.

2.2 Precipitation method

Theoretically, sodium carbonate should react with nickel sulfate in solution to give nickel carbonate and/or hydroxide, which would then during calcination give NiO. Nickel carbonate precipitation never occurs alone but in competition with nickel hydroxide precipitation. In reality, solid phase is generally a mixed complex of nickel hydroxy-carbonates, whose composition probably depends on the carbonate-to-nickel ratio [6]. According to the work of Guillard and Lewis [6], and Patterson et al [7], at pH lower than 9, nickel carbonate salt is the predominating solid phase in the precipitate, while at higher pH values the dominant solid phase is nickel hydroxide. For purpose of this synthesis method it is not that important which phase will be dominant, since they both transform to NiO when heated. It's far more important to be in the region where maximal precipitation can be achieved. Based on the available literature [6, 7], the pH zone of the lowest soluble nickel concentration is estimated to range from 9 to 11.

On the other hand in reaction with ferric nitrate in solution, sodium carbonate should give the same precipitate as sodium hydroxide, ferric hydroxide or hydrated ferric oxide. When heated, it transforms to ferric oxide, which in reaction with nickel oxide at high temperature ($>700 \, ^oC$) produces nickel ferrite.

Furthermore, in this approach there is another reaction taking place, which should be considered. Soluble starch reacts with sodium in alkalization reaction [8]. The reaction itself influences the main reaction only in a way that certain amount of sodium carbonate is lost which should be accounted for. As far as template is concerned, it probably helps the solidification process, since sodium hydroxide is widely used in starch-based adhesives production as gelatinization modifier. The amount of Na_2CO_3 that can be lost in this secondary reaction can be determined using the degree of substitution (DS) [8]. Each monomer unit of starch, anhydro glucose unit (AGU), has three (one primary and two secondary) hydroxyl groups, that can react with sodium. The *DS* is defined as the average number of substituents per AGU and therefore has value between zero and three.

$$DS_t = \frac{n_{A,0}}{n_{AGU,0}}$$

where: $n_{AGU,0}$ – is number of moles of AGU units in the starch and $n_{A,0}$ – is the initial amount of moles of the limiting reactant.

In order to simplify this problem and to avoid deeper analysis of kinetics of this reaction, two possible scenarios were selected. In first, starch reacts with sodium up to the level when degree of substitution equals 1 and the corresponding sample was labeled NF2. In the second, maximal degree of substitution is achieved and the matching sample was labeled NF3. Using chosen values for DS (the theoretically maximal value of 3 and lower value of 1), and number of moles of AGU units in added amount of starch, molar intake of Na_2CO_3 was calculated for both scenarios.

2.3 Synthesis procedure

In the first step of synthesis procedure soluble starch (1g) was added to 100 ml of distilled water, kept at 40-50 ^oC. Upon addition, solution was heated further to boiling point (~100 ^oC), where it was kept for 15 min, and then cooled down to 50-70 ^oC. During the whole process solution was constantly and vigorously stirred by magnetic stirrer. Precursors ($NiSO_4 \times 6H_2O$ and $Fe(NO_3)_3 \times 9H_2O$) were slowly added into the prepared starch/water solution under stirring, in quantities determined by Ni:Fe molar ratio in final product. Mixture was kept at 50-70 ^oC and mixed constantly for next 10 minutes. In case of template route, nothing else was added. Mixture was further stirred for another 10 minutes, and then dried at 80 ^oC until water was evaporated and solid composite was obtained. In case of precipitation route, Na_2CO_3 was added to the mixture, in quantities

calculated from stoichiometric ratios for possible chemical reactions according to two adopted scenarios. As in previous case, mixtures were further stirred for another 10 minutes, and then dried at 80 ºC.

In the final step of both synthesis routes, solid composites were combusted and subsequently calcinated in muffle furnace at 900 ºC, for 5h. Materials produced via precipitation route were additionally rinsed few times with distilled water and centrifuged in order to remove any excess Na_2CO_3.

2.4 Characterization

Structural characterization and phase composition analysis of the prepared Ni-ferrite powders were carried out using X-ray diffraction (XRD). The samples were analyzed at ambient temperature by PANalytical X'Pert PRO MPD X-ray diffractometer using CoK_α radiation. XRD pattern fitting was done using commercial software and database and it yielded mean crystallite size d_{XRD} for a studied phase [9]. [57]Fe Mossbauer spectroscopy (MS) was used for additional phase composition analysis. Mössbauer spectra were taken in a standard transmission geometry at ambient temperature using [57]Co(Rh) source. The calibration was done against α-iron foil data. CONFIT [10] software package was used for fitting and decomposition of the obtained spectra. Microstructure and morphology of the obtained powders was analyzed by scanning electron microscopy (SEM) and field emission scanning electron microscopy (FE-SEM) using JEOL JSM 6610LV and Tescan MIRA3 XM microscopes, respectively. Vibrating sample magnetometer (VSM) with magnetic field strength of 1000 kAm[-1] was used for measurement of room temperature hysteresis loops.

3. Results and discussion

In comparison to template method (sample NF1), pH value of the mixture plays more important role in precipitation route (samples NF2, NF3), influencing both types of Ni solid precipitate (carbonate or hydroxide) to appear and efficiency of precipitation. Hence, pH value was monitored closely through every step of synthesis process.

Prepared starch solution, cooled to 50-70 ºC, prior to addition of inorganic salts has pH value of 5.53. With addition of precursor salts pH of mixture changes to 1.93 due to the acidity of Fe^{3+} hexaaqua ions. Consequent addition of 0.4881 g of sodium carbonate, necessary for the first scenario (sample NF2), increased pH value to 9.83 and brought reactants to the region where nickel hydroxide precipitate should be dominant solid phase and where maximal precipitation is expected. In second case

(sample NF3), addition of 1.1418 g of sodium carbonate, needed for maximal degree of substitution, increased pH value to 10.03, which was still in the preferred pH region.

Morphology of the prepared Ni-ferrite powders is illustrated by corresponding SEM images given in Fig. 1.
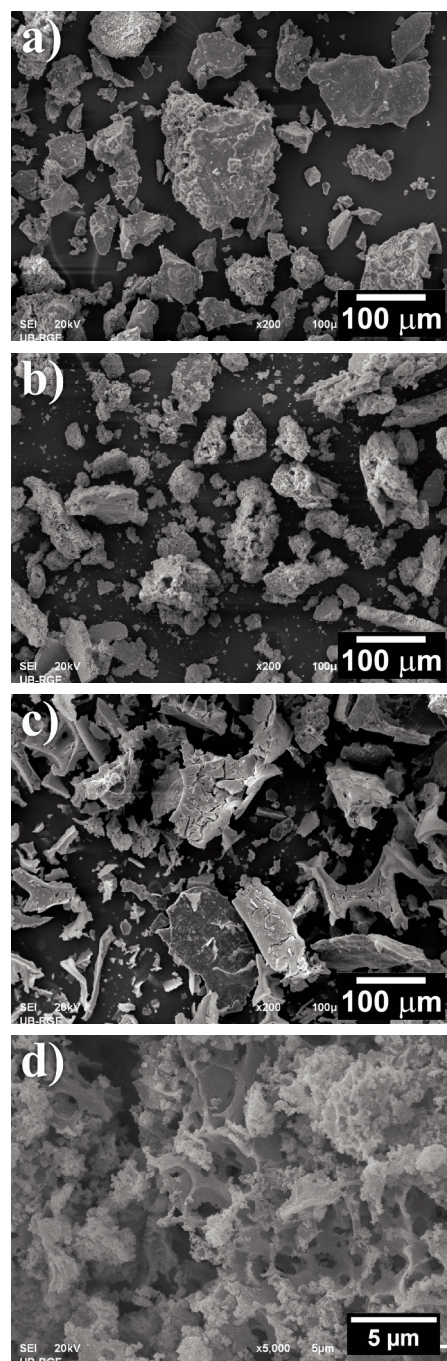

Figure 1. *SEM images of the prepared Ni-ferrite powder samples: a) NF1, b) NF2, c) NF3 and d) NF2 at higher magnification*

As the obtained powders exhibit noticeable differences in microstructure, the influence of preparation method (Na_2CO_3 addition) is evident. The sample produced by template method NF1 (Fig.1a) is significantly less porous than the two samples prepared by precipitation, especially compared to the NF2 sample (Fig.1b) with added amount of Na_2CO_3 calculated for degree of substitution DS = 1. Somewhat lower porosity of sample NF3 (Fig.1c) in relation to sample NF2 (Fig.1b) can be related to larger amount of Na_2CO_3 (DS = 3) and its effect on starch as a gelatinization modifier.

SEM image of the NF2 sample (Fig. 1d) taken at higher magnification illustrates microstructure consisting of porous coral-like network structures. The observed structure corresponds to the shape of interstitial space within the solid starch matrix occupied by precursor solvents. Some of the porosity can be most certainly attributed to the gas formation during the combustion i.e. template removal stage of sample preparation.

FE-SEM images of the prepared Ni-ferrite powders taken at higher magnifications (Fig.2) reveal more-less same fine-grained texture of the network structures. Nevertheless, slight differences in morphology can be observed. The micrograph given in Fig. 2a illustrates microstructure of the NF1 sample that consists of powder particles with the size in the range of 20-70 nm. The microstructure of the sample NF2 is somewhat finer as the particles of about 20 nm can be observed in Fig. 2b. In contrast, Fig. 2c reveals much coarser particles in microstructure of the sample NF3.

Phase composition of the prepared Ni-ferrite powders was analyzed using XRD technique. The obtained X-ray diffractograms of the individual powder samples are given in Fig.3.

According to obtained XRD results (Fig.3) the sample NF1 predominantly consists of $NiFe_2O_4$ phase (ICSD #158834). A single peak which can be observed at $2\theta = 25.5°$ could probably belong to Fe_2O_3. It is possible that at certain Ni to Fe ratio a mixture of $NiFe_2O_4$ and Fe_2O_3 exists. Considering the

similarity of crystal lattices (difference in lattice volume of only $4\cdot10^{-7}$) it is impossible to differentiate between the two phases. Additional small peak at $2\theta = 24.3°$ can be observed that most likely belongs to a phase similar to $Ni(NO_3)_2$, possibly equivalent with Ni-Fe mixture. Moreover, the calculated crystallite size reveals somewhat larger crystallites of 36 nm, which can be associated with the fact that Na_2CO_3 was not used in the preparation process of this sample. In this case the crystallite size was only influenced by reaction kinetics (conditions) and available interstitial space in solid starch matrix.

X-ray diffraction diagram of the sample NF2 reveals monophase composition of the sample, consisting of pure $NiFe_2O_4$ phase (ICSD #158834). Thus, confirming that the precursors were added in
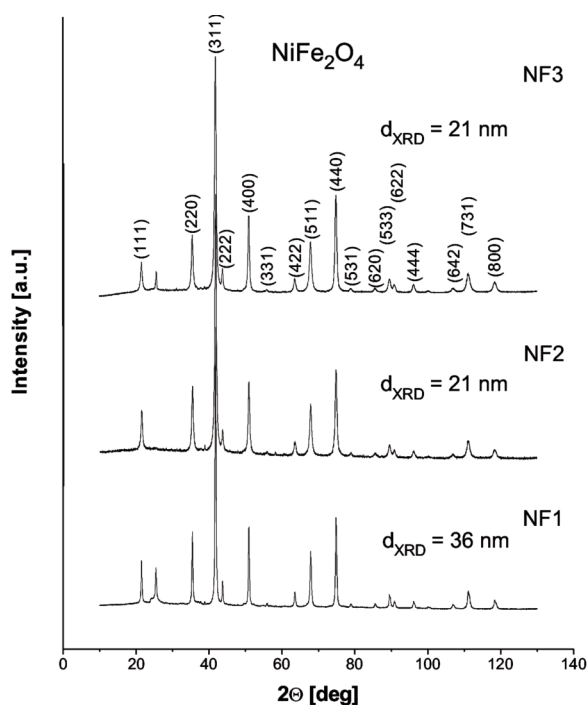

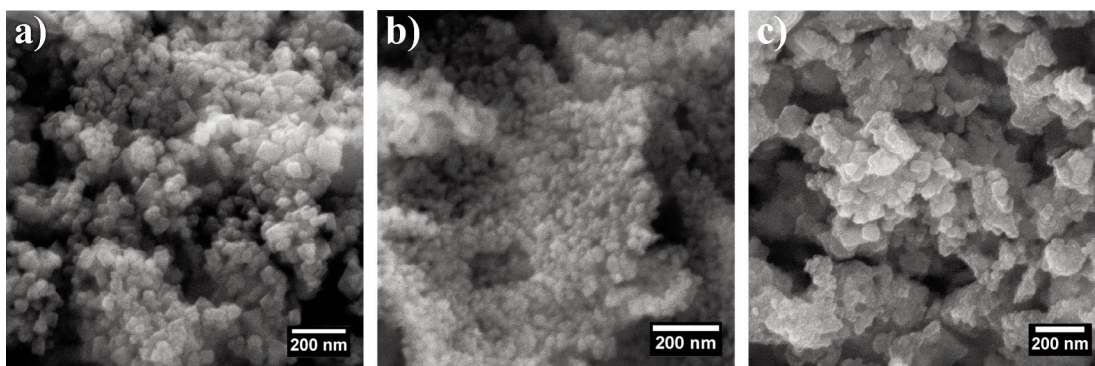*Figure 3. X-ray diffractograms of the studied Ni-ferrite samples*

Figure 2. FESEM images of the obtained Ni-ferrite powders: a) NF1, b) NF2 and c) NF3

stoichiometric amounts. The calculated crystallite size was found to be 21 nm, which is in line with the results of FE-SEM analysis.

Similar to sample NF1 the sample NF3 principally consists of $NiFe_2O_4$ phase with the same peak at $2\theta = 25.5°$. Nonetheless, in contrast to sample NF1 no additional peaks can be observed. The determined mean crystallite size of $d_{XRD} = 21$ nm points up to similar structure compared to the NF2 sample. It seems that larger amount of precipitating agent Na_2CO_3 did not have significant influence on the obtained crystallite size. Particularly, since it is known that Na_2CO_3 retards retrogradation and enhances swelling and solubility of starch [11], and thus could potentially create smaller interstitial space which can be occupied by precursor solvents.

Additional characterization of the prepared nanocrystalline Ni-ferrite powders was carried out by means of ^{57}Fe Mössbauer spectroscopy. The obtained spectra are given in Fig. 4.

Generally speaking, the obtained results of MS analysis support the findings of the microstructural and XRD analysis. Nevertheless, it should be pointed out that the ^{57}Fe Mössbauer spectroscopic analysis is capable of identifying iron containing phases only, so the obtained results can be discussed having this in mind. All three samples (Fig.4) gave characteristic spectra of Ni-ferrite material. As the obtained Mössbauer parameters i.e. isomer shift (IS) and hyperfine field (B_{hf}) listed in Table 1 show very good agreement with the values of room temperature Mössbauer parameters for $NiFe_2O_4$ from the literature [12, 13], corresponding spectral components were assigned to tetrahedral (A) and octahedral (B) Fe^{3+} atom sites.

The observed magnetically split sextets with diminishing intensity and presence of superparamagnetic doublets point to a distribution of crystallite sizes of $NiFe_2O_4$ phase. The observed doublets in the all three room temperature Mössbauer

spectra can be ascribed to superparamagnetism i.e. presence of superparamagnetic fraction of $NiFe_2O_4$ phase, having size less than the critical. According to the literature data [14, 15] the critical particle size for $NiFe_2O_4$ superparamagnetic crystallite is about 10–13 nm. As the thermal energy of such particles can be higher than the anisotropy energy required for switching of the direction of magnetic moment from one easy axis to another it is likely that such particles will exhibit superparamagnetic relaxation [13].

Important effects of the nanocrystalline structure of the studied Ni-ferrites with the size near critical are reduced hyperfine field and reduced magnetization [16, 17]. Unlike the bulk $NiFe_2O_4$ which has collinear ferrimagnetic structure with the magnetization of the tetrahedral and octahedral sublattices set antiparallel to each other, the ultrafine Ni-ferrites were found to have a noncollinear magnetic structure in the surface layers [18]. It is suggested that this surface spin disorder most probably originates from broken exchange bonds as well as high anisotropy or a loss of the long-range order in the surface layer [13]. As the surface area increases with the decrease of the particle size the portion and influence of surface or interface atoms as well as atoms at some irregular positions increases [19].

Table 1. *Obtained Mössbauer paramenters for the studied $NiFe_2O_4$ samples*

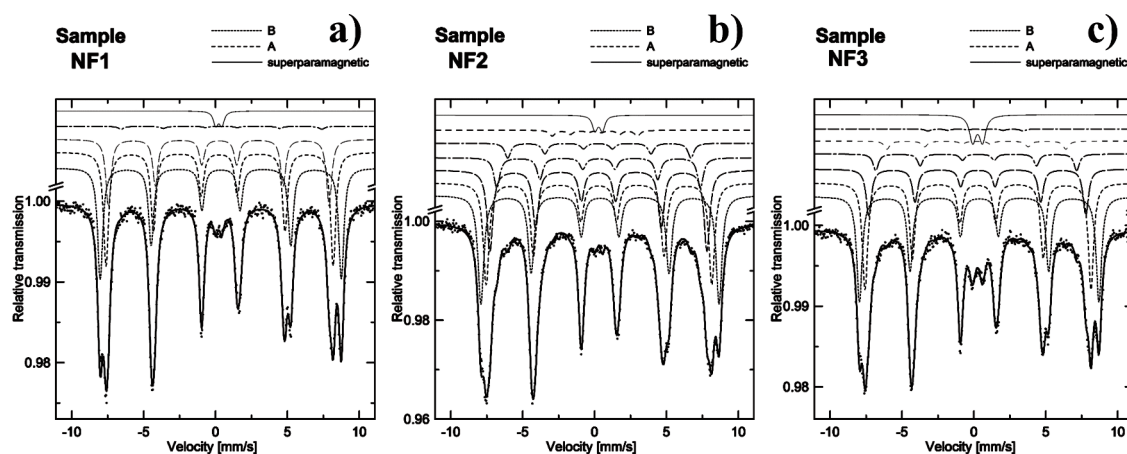| Sample	Component	IS / mm·s^{-1}	B_{hf} / T
NF1	sextet (A)	0.27±0.02	49.1±0.6
	sextet (B)	0.37±0.02	52.1±0.6
NF2	sextet (A)	0.30 ±0.02	48.8±0.5
	sextet (B)	0.38 ±0.02	51.5±0.5
NF3	sextet (A)	0.28 ±0.02	48.8±0.5
	sextet (B)	0.38 ±0.02	51.7±0.5

Figure 4. *Mössbauer spectra of the prepared nanosized Ni-ferrite powders: a) NF1, b) NF2 and c) NF3*

From this point of view, the sample NF1 (Fig.4a) gives the "clearest" spectrum which can be attributed to somewhat larger crystal grains and thus weaker influence of the nanocrystalline component and surface layer atoms. The observed decrease in sextet intensity for the sample NF2 (Fig.4b) and rather small superparamagnetic component can be ascribed to nanocrystalline structure of the material, as determined by XRD, and hence stronger influence of interfaces. The spectrum of the sample NF3 (Fig. 4c), as anticipated, is in line with the XRD results – calculated average crystallite size, as it demonstrates the strongest influence of nanocrystalline component i.e. surface layer atoms.

Magnetic properties of the studied Ni-ferrite materials are illustrated by the obtained hysteresis loops presented in Fig. 5.
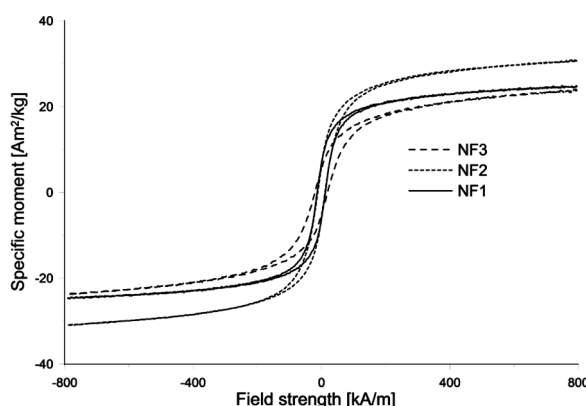

Figure 5. Hysteresis loops of the studied Ni-ferrite samples

In general, there is a strong relation between magnetic behavior and microstructure and morphology i.e. particle size and crystallinity of nanocrystalline Ni-ferrites. The changes in magnetic properties of the these predominantly single phase materials can usually be ascribed to changes in the exchange interactions between tetrahedral and octahedral sub-lattices [20], magneto crystalline and shape anisotropy of crystal, domain size and structure as well as presence of defects i.e. strains [21]. Even so, the presented hysteresis loops (Fig. 5) demonstrate only slight differences between the magnetic properties of the studied materials. This is not entirely unexpected, especially when delicate differences in the structure and phase composition are taken into account. The NF2 sample, prepared with addition of Na_2CO_3 in amount sufficient for degree of substitution DS = 1, exhibits somewhat higher mass magnetization compared to the other two samples. However, such minuscule differences do not leave room for any kind of speculation or any serious discussion. Nonetheless, it can be said that the magnetic properties of the all three prepared Ni-ferrite samples are comparable and

within the expected range for this type of material.

On the other hand, the observed differences in morphology and particle size of the prepared $NiFe_2O_4$ powders can be very significant for other functional properties such as gas-sensing properties. Studies show that adsorption of gases on the surface of material [22], response time [23], sensitivity and response towards certain gases [3] are directly related to particle shape, size and surface to volume ratio. Essentially, small particle size and high specific surface area enhance surface dependant properties like gas-sensing and catalytic efficiency [24].

From that point of view, the NF2 sample probably provides the largest surface to volume ratio as it consists of finest practically single crystal particles. What is more, such particles are useful in producing ferrofluids [25]. In contrast, despite the small crystallite size (21 nm), the FE-SEM images suggest that the NF3 powder consists of fairly larger polycrystalline particles. Such structure of the NF3 sample can be attributed to agglomeration of initially very fine particles [26] and their fusing (sintering) during the calcination stage of sample preparation.

In that sense it can be expected that the differences in performance of the studied samples would become more apparent.

4. Conclusion

The use of soluble starch in synthesis of nanosized $NiFe_2O_4$ was investigated. Two different approaches, template method and precipitation process were explored. The results of SEM microstructural analysis of the prepared Ni-ferrite powders demonstrate the evident influence of the applied preparation method. In contrast, FE-SEM images taken at higher magnifications, show very similar fine-grained network structures of the powders with main difference between them being the size of particles.

According to the obtained XRD results the sample prepared by template method predominantly consists of $NiFe_2O_4$ phase and somewhat larger calculated crystallite size $d_{XRD} = 36$ nm was associated with the fact that the crystallite size was only influenced by reaction conditions and available interstitial space in solid starch matrix. The sample prepared by precipitation process with addition of stoichiometric amount of precipitating agent was found to consist of pure $NiFe_2O_4$ phase with mean calculated crystallite size of 21 nm. The sample prepared by precipitation process with addition of amount of precipitation agent calculated to theoretically maximal value of the degree of substitution principally consists of $NiFe_2O_4$ phase with the phase composition comparable to the template sample. The determined mean crystallite size of 21 nm suggests that larger amount of precipitating agent Na_2CO_3 did not have significant influence on

the obtained crystallite size.

The obtained results of the additional sample characterization by means of ^{57}Fe Mössbauer spectroscopy generally support the findings of the microstructural and XRD analysis. All three samples produced characteristic spectra of Ni-ferrite material. Due to slightly larger crystal grains and thus weaker influence of the nanocrystalline component the template sample gave the "clearest" spectrum. The observed decrease in sextet intensity for the samples prepared by precipitation route and rather small superparamagnetic component were ascribed to the nanocrystalline structure of the material and thus stronger influence of interfaces. The strongest influence of nanocrystalline component atoms was observed for the sample with added maximal amount of precipitation agent.

The obtained room temperature hysteresis loops of the all three prepared Ni-ferrite samples demonstrate only slight differences between the magnetic properties which are comparable and within the expected range for this type of material.

Acknowledgement

References

[1] F. Fresno, T. Yoshida, N. Gokon, Fernández-Saavedra R, Kodama T. International Journal of Hydrogen Energy, 35 (16) (2010) 8503-8510.

[2] K. Lin, A.K. Adhikari, Z. Tsai, Y. Chen, T. Chien, H. Tsai. Catalysis Today, 174 (1) (2011) 88-96.

[3] S.L. Darshane, S.S. Suryavanshi, I.S. Mulla. Ceramics International, 35 (5) (2009) 1793-1797.

[4] D.T.T. Nguyet, N.P. Duong, L.T. Hung, T.D. Hien, T. Satoh., 509 (23) (2011) 6621-6625.

[5] Marinca TF, Chicinaş I, Isnard O, Pop V, Popa F. Journal of Alloys and Compounds, 509 (30) (2011) 7931-7936.

[6] Guillard D, Lewis AE. Industrial & Engineering Chemistry Research, 40(23) (2001) 5564-5569.

[7] J.W. Patterson, H.E. Allen, J.J. Scala, Water Pollution Control Federation, 49 (12) (1977) 2397-2410.

[8] Z. Dong-fang, JU Ben-zhi, Z. Shu-fen, Y. Jin-zong, Proc. 3rd International Conference on Functional Molecules ICFM, 8-11 September, Dalian, China, 2005, p. 25-30.

[9] X'Pert High Score Plus 2.0a, PANalytical BV, Lelyweg 1, Almelo, the Netherlands. ICSD Database release 2010/2, FIZ Karlsruhe, Germany.

[10] Žák T, Jirásková Y. Surface and Interface Analysis, 38(4) (2006) 710-714.

[11] A. Mohamed, B. Jamilah, K.A. Abbas, R.A. Rahman, K. Roselina, Am. J. Agr. Bio. Sci., 3(4) (2008) 639-646.

[12] V. Šepelák, D. Baabe, D. Mienert, D. Schultze, F. Krumeich, F.J. Litterst, K.D. Becker, J. Magn. Magn. Mater., 257(2-3) (2003) 377-386.

[13] J. Jacob, A.M. Khadar. Journal of Applied Physics, 107 (11) (2010) 114310.

[14] H. Yang, L. Zhao, X. Yang, L. Shen, L. Yu, W. Sun, Y. Yan, W. Wang, S. Feng, J. Magn. Magn. Mater. 271(2-3) (2004) 230-236.

[15] T. Komatsu, N. Soga. Journal of Applied Physics, 51 (1) (1980) 601-606.

[16] D. Lin, A.C. Nunes, C.F. Majkrzak, A.E. Berkowitz, J. Magn.Magn. Mater., 145(2) (1995) 343-348.

[17] R. Kodama, A. Berkowitz, J.E. Mcniff, S. Foner,. Physical Review Letters, 77 (2) (1996) 394-397.

[18] K. Haneda, Can. J. Phys. 65 (1987) 1233-1244.

[19] J.-M. Grenèche, M. Miglierini, in Mössbauer Spectroscopy in Materials Science, Eds. (M. Miglierini, D. Petridis), Kluwer, Dordrecht, 1999.

[20] A. Pradeep, Priyadharsini P, Chandrasekaran G. Materials Chemistry and Physics, 112 (2) (2008) 572-576.

[21] A.B. Nawale, N.S. Kanhe, K.R. Patil, S.V. Bhoraskar, V.L. Mathe, A.K. Das,. Journal of Alloys and Compounds, 509 (12) (2011) 4404-4413.

[22] L. Yang, Y. Xie, H. Zhao, X. Wu, Y. Wang,. Solid-State Electronics, 49(6) (2005) 1029-1033.

[23] G.F. Fine, L.M. Cavanagh, A. Afonja, R. Binions,. Sensors (Basel), 10(6) (2010) 5469-502.

[24] L. Ma, L. Chen, S. Chen,. Materials Chemistry and Physics, 114 (2-3) (2009) 692-696.

[25] R. Ahmadi and H. R. Madaah Hosseini, Journal of Mining and Metallurgy, Section B: Metallurgy, 48 (1) B (2012) 81-88.

[26] J. Sopousek, J.Bursik, J. Zalesak and Z. Pesina, Journal of Mining and Metallurgy, Section B: Metallurgy, 48 (1) B (2012) 63-71.